

TraSw: Tracklet-Switch Adversarial Attacks against Multi-Object Tracking

Delv Lin*, Qi Chen*, Chengyu Zhou*, Kun He†

School of Computer Science and Technology
Huazhong University of Science and Technology

{derrylin, bloom24, hust_zcy, brooklet60}@hust.edu.cn

Abstract

Benefiting from the development of Deep Neural Networks, Multi-Object Tracking (MOT) has achieved aggressive progress. Currently, the real-time Joint-Detection-Tracking (JDT) based MOT trackers gain increasing attention and derive many excellent models. However, the robustness of JDT trackers is rarely studied, and it is challenging to attack the MOT system since its mature association algorithms are designed to be robust against errors during tracking. In this work, we analyze the weakness of JDT trackers and propose a novel adversarial attack method, called Tracklet-Switch (TraSw), against the complete tracking pipeline of MOT. Specifically, a push-pull loss and a center leaping optimization are designed to generate adversarial examples for both re-ID feature and object detection. TraSw can fool the tracker to fail to track the targets in the subsequent frames by attacking very few frames. We evaluate our method on the advanced deep trackers (i.e., FairMOT, JDE, ByteTrack) using the MOT-Challenge datasets (i.e., 2DMOT15, MOT17, and MOT20). Experiments show that TraSw can achieve a high success rate of over 95% by attacking only five frames on average for the single-target attack and a reasonably high success rate of over 80% for the multiple-target attack. The code is available at <https://github.com/DerryHub/FairMOT-attack>.

1. Introduction

Multiple Object Tracking (MOT) has been dramatically boosted in recent years due to the rapid development of Deep Neural Networks (DNNs) [1, 2, 27], and has a wide range of applications, such as autonomous driving, intelligent monitoring, human-computer interaction, etc. The deep MOT trackers can be divided into two main categories: Detection-Based-Tracking (DBT) trackers [4, 19, 21, 31] and Joint-Detection-Tracking (JDT) trackers [25, 33, 34]. Con-

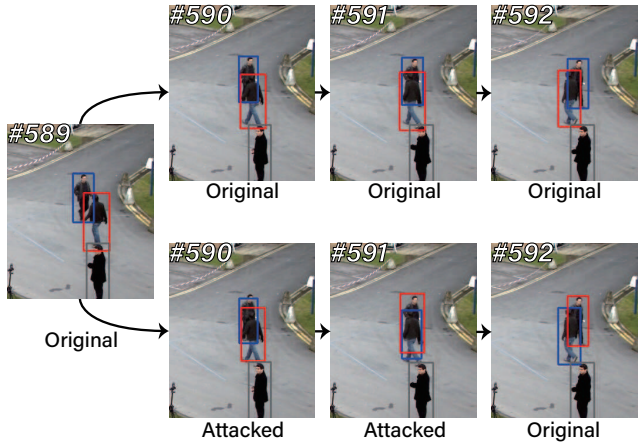


Figure 1. By perturbing only two frames in this example video, we can exchange the 19th ID and the 24th ID completely. Starting from frame 592, the 19th and 24th IDs can keep the exchange without noise. *First row*: the original video clip. *Second row*: the adversarial video clip. The blue boxes represent the 19th ID, the red boxes represent the 24th ID, and the gray boxes denote the 16th ID not participated in the attack.

sidering JDT trackers generally have faster speed and higher accuracy than DBT trackers, they remain dominant in the field of real-time multiple object tracking.

On the other hand, numerous works have been proposed for the adversarial attacks on deep learning models in computer vision. Szegedy *et al.* first discovered the existence of adversarial examples for image classification [24]. Their work shows that modern DNN models are highly vulnerable to adversarial examples, which are images with perturbations imperceptible to the human visual system [22, 24]. Studying adversarial attacks can improve the understanding of DNNs and find the potential risks of the systems. Researches on adversarial learning are mainly focused on the image classification [24] and eventually spread out to other tasks, including face recognition [8, 30], object detection [17, 26, 28] and semantic segmentation [11, 28]. To our

* Equal contribution. † Corresponding author.

knowledge, the vulnerability of MOT trackers is rarely studied. In this work, we will address the security of MOT and focus on attacking JDT trackers.

Unlike the image classification or object detection tasks, MOT aims to track all targets of interest in continuous video sequences and builds their moving trajectories. A typical JDT tracker addresses the problem in two steps [25]. Firstly, the tracker locates objects of interest and extracts their features for each frame in the video. Then, according to a specific similarity metric, each detected object is associated with a trajectory. The continuous tracking process allows the tracker to save trajectories’ motion and appearance information in tracklets for a long period (i.e., 30 frames) to make more precise decision [25]. It means the detection-based attack methods [17, 26, 28] that blind the target object detection need to attack successfully and continuously for much more frames to fool the tracker, as shown by our experiments in Sec. 4.3. Besides, though the association between objects and existing trajectories is indeed a classification problem, it considers both the motion and appearance information. It is hard to define an optimization objective to generate adversarial examples. Especially the motion information is discrete.

In this work, we study the adversarial attacks against JDT trackers and propose a novel attack method called the *Tracklet-Switch* (TraSw) consisting of the *PushPull* and the *CenterLeaping* technique. TraSw can fool the tracker by attacking as few as one frame. In a nutshell, our method learns an effective perturbation generator to make the tracker confuse intersecting trajectories, which is a very common scene in MOT, especially pedestrian tracking. Specifically, we analyze the association algorithm, which combines appearance and motion distance as the similarity cost matrix. It is explicit that when the detected objects overlap each other, the tracker identifies which trajectory the object belongs to by comparing its appearance with trajectories’ appearances. In order to involve the past appearance information and mitigate the impact of a single frame, the tracker uses a smooth feature representing a trajectory’s appearance. As frames go by, the past appearance’s influence dismiss. Based on this observation, the attacker deliberately reforms the feature embedding of the overlapping objects to make them similar to the other trajectory’s appearance [25] but be further to the origin. During this process, the appearances of these two trajectories are silently modified and switched. As a result, the tracker may track a completely different object without realizing this error. An example is shown in Fig. 1.

Our main contributions can be summarized as follows:

- We are the first to study adversarial attacks against JDT trackers. A novel and efficient TraSw method is proposed to deceive advanced JDT trackers by only a few frames attacked in the videos.
- Numerous experiments on MOT-Challenge datasets demonstrate that our method can efficiently fool JDT trackers using *PushPull* on re-ID branch and *CenterLeaping* on detection branch.
- Our method has excellent transferability to DBT trackers. Experimental results show that the state-of-the-art (SOTA) DBT tracker (e.g., ByteTrack [32]) can also be deceived by TraSw, even though it is not specially designed for DBT trackers.

2. Related Work

2.1. Multiple Object Tracking

Multiple object tracking (MOT) aims to locate and identify the targets of interest in the video, and then estimate their movements in the subsequent frames [19], such as pedestrians on the street, vehicles on the road, and animals on the ground.

The mainstream MOT trackers are divided into Detection-Based-Tracking (DBT) trackers [4, 19, 21, 31] and Joint-Detection-Tracking (JDT) trackers [25, 33, 34]. The DBT trackers break tracking down to two steps: 1) the detection stage, in which targets are localized; 2) the association stage, where the targets are linked to existing trajectories. However, the DBT trackers are inefficient and not optimized end-to-end due to the two-step processing. To address this problem, [25] designed the first JDT tracker, JDE, meeting the real-time performance without losing accuracy. Incorporating the appearance embedding model into a single-shot detector to simultaneously output the detections and embeddings, JDE accomplishes the end-to-end training and proposes an effective association method.

The association problem of MOT is regarded as a bipartite matching problem [13, 25] based on the similarity between the detected objects and the trajectories. The tracker used tracklets to maintain the appearance and motion states of trajectories. In the first frame, the tracker recognizes objects, numbers the trajectories in order, and saves their states as the initial tracklets. Then for a coming frame, the tracker compares each detected object with tracklets to determine whether it belongs to an existing trajectory or is a new trajectory. After that, the tracker updates trajectory information with the current frame (i.e., updates tracklets). In the meantime, the tracker also needs to estimate the current trajectories. When a tracklet isn’t updated for consecutive R frames (i.e., 30 frames), the tracklet will be deleted, and the tracking of this trajectory is terminated. Even if the corresponding tracking object reappears after R frames, it is regarded as a new trajectory.

So far, JDT method is used in most real-time scenarios and inspires many outstanding models. Our primary target model is one of the famous and widely used models, FairMOT [33].

2.2. Adversarial Attacks

CNN models are known to be vulnerable to adversarial examples, since the first discovery of the adversarial examples in 2014 [24]. After that, numerous adversarial attack methods have been proposed [5, 7, 10, 18, 20]. Most of the adversarial attack researches are mainly focused on the basic computer visual task of image classification. To our knowledge, the adversarial attack research in Visual Object Tracking systems is scarce, especially in Multiple Object Tracking systems.

Recently, there have been several explorations of adversarial attacks against the Single Object Tracking (SOT) [3, 12, 29], which aims at tracking a determined object in the video sequences. Chen *et al.* [3] propose the first one-shot attack method by adding perturbations on the target path in the initial frame to make the tracker lose the target in the subsequent frames. Meanwhile, Yan [29] propose a *cooling-shrinking* attack method to fool the SiamPRN-based trackers [15, 16], which can cool hot regions on the heatmap and shrink the size of predicted bounding box, so as to make the target invisible to the trackers. Most recently, Jia *et al.* [12] present a decision-based black-box attack to decrease the IoU scores gradually.

For the MOT system, *tracker hijacking* [13] is the first adversarial attack method to deceive the DBT tracker in automatic driving. It uses adversarial examples generated on objection detection, which fabricates a bounding box toward the expected attacker-specified direction and erase the original bounding box. It makes the tracker assign an error velocity to the attacked tracklet, thus resulting in the detected object being too far from the tracklet’s expectation to be associated.

3. The TraSw Attack

In this section, we propose a novel method called the *Tracklet-Switch* (TraSw) attack against the JDT trackers. Our method finds two intersecting trajectories to make their tracklets switch. Representatively, we choose FairMOT [33] as our main target model, but our method can also be adopted to attack other JDT trackers, even DBT trackers.

3.1. Overview of FairMOT

FairMOT stands out among many JDT trackers by achieving a good trade-off between accuracy and efficiency. As shown in Fig. 2a, the network architecture consists of two homogeneous branches for the object detection and feature extraction. The online association also plays an essential role in FairMOT, as shown in Fig. 2b.

Detection Branch. The anchor-free detection branch of FairMOT is built on CenterNet [9], consisting of the heatmap head, center-offset head and box-size head. We denote the ground-truth (GT) bounding box of the i -th object

in the t -th frame as $box_t^i = (x_1^{t,i}, y_1^{t,i}, x_2^{t,i}, y_2^{t,i})$. Object i ’s center $(c_x^{t,i}, c_y^{t,i})$ is computed by $c_x^{t,i} = \frac{x_1^{t,i} + x_2^{t,i}}{2}$ and $c_y^{t,i} = \frac{y_1^{t,i} + y_2^{t,i}}{2}$. The response location of the bounding box’s center on the heatmap can be obtained by dividing the stride (which is 4 in FairMOT) $(\lfloor \frac{c_x^{t,i}}{4} \rfloor, \lfloor \frac{c_y^{t,i}}{4} \rfloor)$. The heatmap value indicates the probability of the presence of an object centering in the corresponding location. The GT box size and center offset is computed by $(x_2^{t,i} - x_1^{t,i}, y_2^{t,i} - y_1^{t,i})$ and $(\frac{c_x^{t,i}}{4} - \lfloor \frac{c_x^{t,i}}{4} \rfloor, \frac{c_y^{t,i}}{4} - \lfloor \frac{c_y^{t,i}}{4} \rfloor)$, respectively.

Re-ID Branch. The re-ID branch generates the re-ID features to distinguish the objects. Denote the feature map as $feat_t \in \mathbb{R}^{512 \times H \times W}$. The re-ID feature $feat_t^i \in \mathbb{R}^{512}$ represents the feature vector of the i -th object, whose L_2 norm equals 1.

Association. FairMOT follows the standard online association algorithm in [25]. The tracker maintains a tracklet pool TrP_t containing all the valid tracklets before the $t+1$ -th frame. A tracklet describes the appearance state a_t^i and motion state $m_t^i = (x^{t,i}, y^{t,i}, \gamma^{t,i}, h^{t,i}, \dot{x}^{t,i}, \dot{y}^{t,i}, \dot{\gamma}^{t,i}, \dot{h}^{t,i})$ of the i -th trajectory in the t -th frame. The a_0^i is initialized with the appearance embedding $feat_0^i$ and updated by:

$$a_t^i = \alpha \cdot a_{t-1}^i + (1 - \alpha) \cdot feat_t^i, \quad (1)$$

where $feat_t^i$ is the appearance embedding of the matched object in the t -th frame. The bounding box information of m_t^i is updated by the predicted center $x^{t,i}, y^{t,i}$, aspect ratio $\gamma^{t,i}$ and height $h^{t,i}$ in the t -th frame, and velocity information $(\dot{x}^{t,i}, \dot{y}^{t,i}, \dot{\gamma}^{t,i}, \dot{h}^{t,i})$ is updated by the Kalman filter. For a coming frame, we can compute the similarity between the

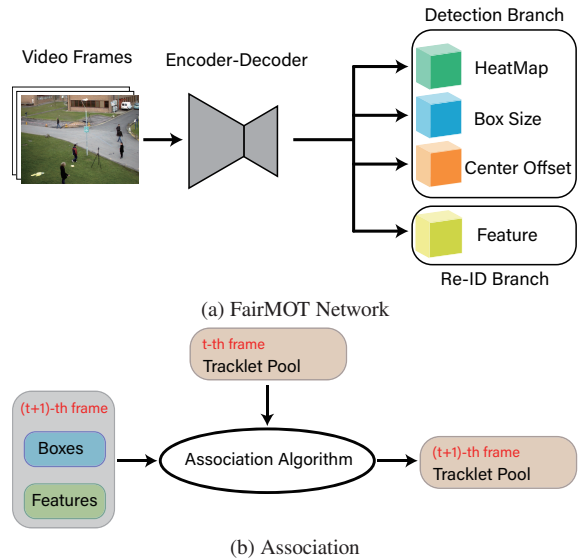


Figure 2. Overview of FairMOT.

observed objects in the current t -th frame and all the tracklets in the $(t-1)$ -th frame.

Then the association problem is solved by the Hungarian algorithm using the final cost matrix:

$$d_t = \lambda \cdot d_{box}(K(m_{t-1}), box_t) + (1 - \lambda) \cdot d_{feat}(a_{t-1}, feat_t), \quad (2)$$

where box_t and $feat_t$ denote the detected bounding boxes and the features in the t -th frame, $K(\cdot)$ represents the Kalman filter which uses tracklets to predict the corresponding trajectories' expected positions in the t -th frame, $d_{box}(\cdot)$ stands for a certain measurement of the spatial distance, and $d_{feat}(\cdot)$ represents the cosine similarity.

3.2. Problem Definition

Let $V = \{I_1, \dots, I_t, \dots, I_N\}$ denote a video containing N frames. In simple terms, there are two intersecting trajectories observed by the tracker $f_\theta(\cdot)$. Denote the two trajectories as $T_i = \{O_{s_i}^i, \dots, O_t^i, \dots, O_{e_i}^i\}$ and $T_j = \{O_{s_j}^j, \dots, O_t^j, \dots, O_{e_j}^j\}$ respectively, that are adjacent in the t -th frame. Their bounding boxes and features are $B_k = \{box_{s_k}^k, \dots, box_t^k, \dots, box_{e_k}^k\}$ and $F_k = \{feat_{s_k}^k, \dots, feat_t^k, \dots, feat_{e_k}^k\}$ for $k \in \{i, j\}$, $box \in \mathbb{R}^4$ and $feat \in \mathbb{R}^{512}$.

In the following, we define the adversarial video as $\hat{V} = \{I_1, \dots, I_{t-1}, \hat{I}_t, \dots, \hat{I}_{t+n-1}, I_{t+n}, \dots, I_N\}$, where I, \hat{I} indicates the original frame and the adversarial frame, respectively. We define the problems of single-target attack and multiple-target attack as follows:

1. **Single-Target Attack.** For an attack trajectory T_i , we call T_j , that is overlapping with T_i in the t -th frame, the screener trajectory. The adversarial video \hat{V} misleads the tracker to estimate the trajectory as $\hat{T}_i = \{O_{s_i}^i, \dots, O_{t-1}^i, O_t^j, \dots, O_{t+n-1}^j, O_{t+n}^i, \dots, O_{e_j}^j\}$. The single-target attack aims to add adversarial perturbations from the t -th to at most the $(t+n-1)$ -th frames such that the tracking of trajectory T_i is changed to that of T_j wrongly since the t -th frame.

2. **Multiple-Target Attack.** Similarly, the multiple-target attack aims to craft the adversarial video \hat{V} such that all the pairwise trajectories that are overlapping with other are predicted wrongly since their overlapping frames.

3.3. Feature Attack with Push-Pull Loss

The JDT tracker distinguishes the objects through a combination of motion and appearance similarity. So when objects are close to each other, the tracker relies heavily on the features to distinguish the objects. Inspired by the triplet

loss [23], we design the *PushPull* loss as follows:

$$\mathcal{L}_{pp}(a_{t-1}^k, feat_t^k, feat_t^{\tilde{k}}) = d_{feat}(a_{t-1}^k, feat_t^k) - d_{feat}(a_{t-1}^k, feat_t^{\tilde{k}}), \quad (3)$$

where $d_{feat}(\cdot)$ denotes the cosine similarity, a_{t-1}^k represents the appearance state of the attack tracklet k (k represents the attack trajectory's ID), \tilde{k} represents the screener's trajectory that overlaps most with trajectory k , and $feat_t^k$ represents the feature of trajectory k in the t -th frame. The loss will make $feat_t^k$ dissimilar to tracklet k and make $feat_t^{\tilde{k}}$ similar to tracklet k .

Specifically, in FairMOT, the object's feature is extracted from the feature map $feat_t \in \mathbb{R}^{512 \times H \times W}$ according to the predicted object center (x, y) . Considering that the surrounding locations of the center may be activated, we calculate the appearance cost within a nine-block box location for a more stable attack. So the *PushPull* loss for the single-target attack against FairMOT is as follows:

$$\mathcal{L}_{pp}^s = \sum_{k \in \{i, j\}} \sum_{(dx, dy) \in \mathcal{B}} \mathcal{L}_{pp}(a_{t-1}^k, feat_t^{k, (dx, dy)}, feat_t^{\tilde{k}, (dx, dy)}), \quad (4)$$

where \mathcal{B} indicates a set of offsets in the nine-block box location, as illustrated in Fig. 3b; \tilde{k} denotes the trajectory that overlaps most with trajectory k (i.e., $\tilde{i} = j$ and $j = i$), and $feat_t^{k, (dx, dy)}$ represents the feature according to the position around the center of trajectory k .

The *PushPull* loss for the multiple-target attack against FairMOT is as follows:

$$\mathcal{L}_{pp}^m = \sum_{i \in \mathcal{S}_t} \sum_{k \in \{i, \tilde{i}\}} \sum_{(dx, dy) \in \mathcal{B}} \mathcal{L}_{pp}(a_{t-1}^k, feat_t^{k, (dx, dy)}, feat_t^{\tilde{k}, (dx, dy)}), \quad (5)$$

where \mathcal{S}_t represents a collection of trajectory IDs that could be attacked in the t -th frame.

3.4. Detection Attack with Center Leaping

Attacking the features of intersecting trajectories can generally fool the tracker. However, it is insufficient when the two boxes are too far. As the bounding boxes are computed with discrete locations of heat points in the heatmap, we cannot directly optimize a bounding box's loss to make the objects close to each other.

In order to reduce the distance between the objects, we propose a novel and simple method, called the *CenterLeaping*. The optimization objective can be summarized as reducing the IoU between the screener tracklet's predicted box and the attack trajectory's detected box. The goal is achieved by reducing the distance between their centers, as

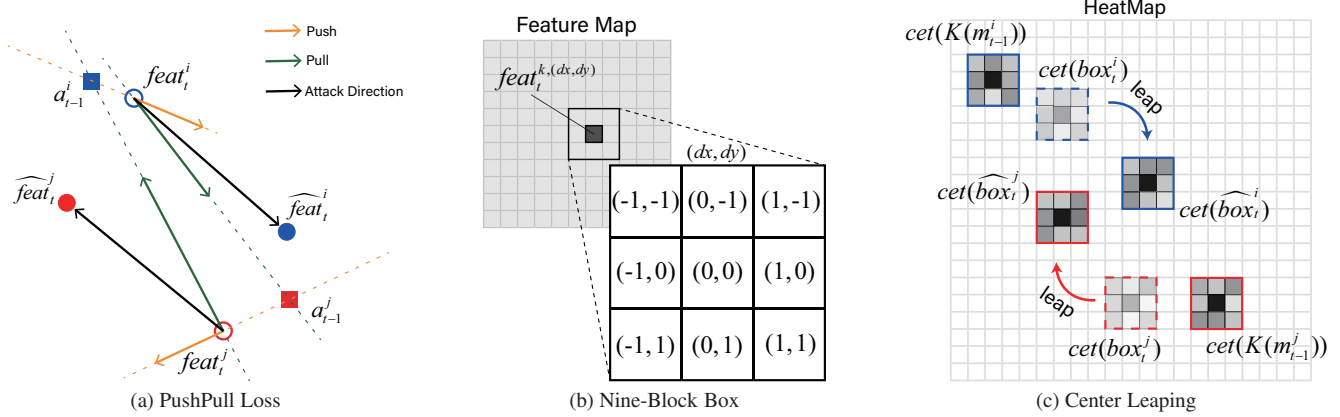


Figure 3. Key factors in the proposed TraSw method. (a) The effect of the *PushPull* loss. The blue and red points represent different IDs that will be attacked to exchange. The goal of the *PushPull* loss is to push the i -th feature in the t -th frame, $feat_t^i$, away from its smooth feature in the $(t-1)$ -th frame, a_{t-1}^i , and to pull $feat_t^i$ to be close to another smooth feature in the $(t-1)$ -th frame, a_{t-1}^j ; and vice versa to $feat_t^j$. (b) The nine-block box (\mathcal{B}). The surrounding features are also added to calculated the loss. (c) The center leaping for the detection branch. The dotted boxes indicate the original heat points, which need to be cooled down; and the solid boxes in the t -th frame indicate the adversarial heat points, which need to be heated up. In this way, the $cet(box_t^i)$ and $cet(box_t^j)$ leaps to $cet(\widehat{box}_t^i)$ and $cet(\widehat{box}_t^j)$ along the direction of $cet(K(m_{t-1}^i))$ and $cet(K(m_{t-1}^j))$, respectively.

well as the differences of their sizes and offsets. Hence, the optimization function for box_t^k can be expressed as follows:

$$\begin{aligned} & \min \sum_{k \in \{i,j\}} IoU(K(m_{t-1}^{\tilde{k}}), box_t^k) \\ & = \min \sum_{k \in \{i,j\}} \left(d_{cet}(cet(K(m_{t-1}^{\tilde{k}})), cet(box_t^k)) + \right. \\ & \quad d_{size}(size(K(m_{t-1}^{\tilde{k}})), size(box_t^k)) + \\ & \quad \left. d_{offset}(off(K(m_{t-1}^{\tilde{k}})), off(box_t^k)) \right), \end{aligned} \quad (6)$$

where $cet(\cdot)$ computes the center of a box, $size(\cdot)$ represents the box size, and $off(\cdot)$ denotes the box offset.

In order to make the detected center of trajectory k to be close to $cet(K(m_{t-1}^{\tilde{k}}))$, based on the focal loss of FairMOT, we design the *CenterLeaping* loss as follows:

$$\begin{aligned} \mathcal{L}_{cl} = & \sum_{k \in i,j} \left(\sum_{(x,y) \in \mathcal{B}_{c_k}} -(1 - HM_{x,y})^\gamma \log(HM_{x,y}) + \right. \\ & \left. \sum_{(x,y) \in \mathcal{B}_{c_{\nearrow \tilde{k}}}} -(HM_{x,y})^\gamma \log(1 - HM_{x,y}) \right), \end{aligned} \quad (7)$$

where i and j denotes the two most overlapping trajectories in the t -th frame, $HM_{x,y}$ means the value of heatmap at location (x, y) , c_k represents the center of the trajectory k , $c_{\nearrow \tilde{k}}$ represents the point which is in the direction from c_k to $cet(K(m_{t-1}^{\tilde{k}}))$ as shown in Fig. 3c. In the optimization iteration, the point $c_{\nearrow \tilde{k}}$ will leap to the next grid along the direction until the attack succeeds. As a result, the heatmap values on the original centers' positions are cooled down, while the points closer to $cet(K(m_{t-1}^{\tilde{k}}))$ are heated up.

In addition, the widths and heights of bounding boxes should not be overlooked due to Eq. (6). We restrain the sizes and offsets of the objects by a Smooth L_1 regression loss:

$$\begin{aligned} \mathcal{L}_{reg} = & \mathcal{L}_{size} + \mathcal{L}_{offset} \\ = & \sum_{k \in i,j} \sum_{(x,y) \in \mathcal{B}} d_{size}(size(K(m_{t-1}^{\tilde{k}})), size(box_t^k)) + \\ & \sum_{k \in i,j} \sum_{(x,y) \in \mathcal{B}} d_{offset}(off(K(m_{t-1}^{\tilde{k}})), off(box_t^k)), \end{aligned} \quad (8)$$

where d_{size} and d_{offset} both use the Smooth L_1 loss.

3.5. Generating the Adversarial Video

With the summation of all the loss functions, we can get the final optimization objective function:

$$\min_{\tilde{V}} Loss = \min_{\tilde{V}} \mathcal{L}_{pp} + \mathcal{L}_{cl} + \mathcal{L}_{reg}. \quad (9)$$

To conceal the disturbance, we restrain the L_2 distance between the adversarial images \hat{I} and the original images I . Then we could get the adversarial images \hat{I} as follows:

$$\hat{I}_0 = I, \hat{I}_{k+1} = Clip_I^{[0,1]} \left(\hat{I}_k + \frac{\nabla_{\hat{I}} Loss(\hat{I}_k; \theta)}{\|\nabla_{\hat{I}} Loss(\hat{I}_k; \theta)\|_2} \right), \quad (10)$$

where \hat{I}_k denotes the k -th iteration of optimization.

The algorithm overview of crafting the adversarial videos is shown in Algorithm 1. Take the single-target attack as an example, we specify an attack trajectory, ID_{att} , in the original tracking video before the attack. Then for each coming frame, we initialize the tracklet pools, TrP_t

Algorithm 1: TraSw Attack

Input: Video image sequence $V = \{I_1, \dots, I_N\}$; MOT Tracker(\cdot);
Input: Attack ID ID_{att} ; Attack IoU threshold Thr_{IoU} ;
Start attack frame Thr_{frame} ; Maximum iteration Thr_{iter} .
Output: Sequence of adversarial video \hat{V} ; Original tracklet pool TrP_N ; Adversarial tracklet pool \hat{TrP}_N .

```
1 Init  $\hat{V} \leftarrow \{\}$ ;  $TrP_0 \leftarrow None$ ;  $\hat{TrP}_0 \leftarrow None$ .
2 for  $t=1$  to  $N$  do
3    $TrP_t \leftarrow Tracker(I_t, TrP_{t-1})$ ;
4    $\hat{TrP}_t \leftarrow Tracker(I_t, \hat{TrP}_{t-1})$ ;
5    $\hat{I}_t \leftarrow I_t$ ;  $\triangleright$  initialize the outputs;
6   if  $Exist(ID_{att}, TrP_t) > Thr_{frame}$  and
      $CheckFit(TrP_t|ID_{att}, \hat{TrP}_t|ID_{att})$  then
7      $ID_{scr} \leftarrow FindMaxIoU(TrP_t, ID_{att})$ ;
8     if  $IoU(TrP_t|ID_{att}, TrP_t|ID_{scr}) > Thr_{IoU}$ 
        then
9        $noise \leftarrow NoiseGenerator(ID_{att}, ID_{scr},$ 
           $I_t, TrP_t, \hat{TrP}_{t-1}, Tracker(\cdot), Thr_{iter})$ ;
10       $\hat{I}_t \leftarrow C_{ilp}[0,1](I_t + noise)$ ;
11       $\triangleright$  clip the adversarial image to  $[0, 1]$ ;
12       $\hat{TrP}_t \leftarrow Tracker(\hat{I}_t, \hat{TrP}_{t-1})$ ;
13       $Thr_{IoU} \leftarrow 0$ ;
14       $\triangleright$  set  $Thr_{IoU}$  to 0 if start to attack;
15    end
16  end
17   $\hat{V} \leftarrow \hat{V} \cup \hat{I}_t$ ;  $\triangleright$  update the adversarial video;
18 end
```

and \hat{TrP}_t , with the original frame, and also initialize the adversarial frame \hat{I}_t as I_t . Then we conduct a double check to determine whether to attack the current frame: (1) whether the object of the trajectory ID_{att} has appeared for more than Thr_{frame} frames; (2) whether the tracking of the attack object is correct. If both checks are passed, we find the object that overlaps with the trajectory ID_{att} mostly and get the corresponding screener trajectory, ID_{scr} . Then we check whether the IoU between the trajectories, ID_{att} and ID_{scr} , is greater than Thr_{IoU} . If it is true, the current frame will be attacked.

We generate the noise by optimizing Eq. (9) iteratively until the tracker makes mistakes in the current frame or the iterations reaches Thr_{iter} (60 in default). Note that during the course of generation, point $c_{\nearrow k}$ will jump to the next grid closer to c_k at certain number of iterations as presented in Sec. 3.4. The noise is then added to the original frame by Eq. (10). We believe the noise should be added to the current frame no matter the attack succeeds or not, and the experiments in Sec. 4.3 show that such action contributes to an easier attack for the following frames. The tracklet pool

\hat{TrP}_t is then re-updated by the adversarial frame \hat{I}_t , and the threshold Thr_{IoU} is set to zero. In the end, the adversarial frame \hat{I}_t is added to the adversarial video \hat{V} .

4. Experiments and Discussions

4.1. Experimental Setup

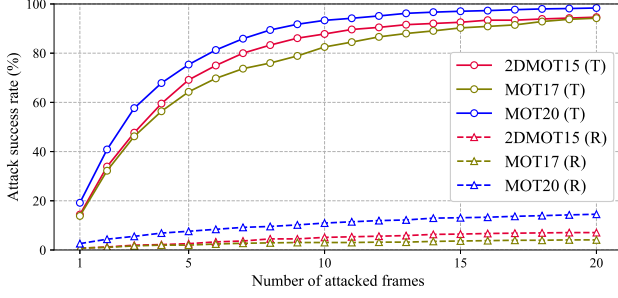
Attacked Models and Datasets. We choose two representative JDT-based trackers as the target models: FairMOT [33] and JDE [25]. FairMOT is also used as the model for ablation studies. We validate the proposed TraSw attack method on the MOT-Challenge test datasets: 2DMOT15 [14], MOT17 [21] and MOT20 [6]. As there is no available attack method for the MOT attack in the same scenario, we compare our method with the baseline of adding random noise, denoted as RanAt, whose L_2 distances are limited to $[2, 8]$ randomly.

Evaluation Metric. We define an attack to be successful if the detected objects of the attack trajectory are no longer associated with the original tracklets after the attack. As described in Sec. 3.5, our method attacks when an object overlaps with the attack object. So the calculation of the attack success rate depends on two factors. Firstly, we need to obtain the number of trajectories meeting the attack conditions: (1) the trajectory's object should have appeared for at least Thr_{frame} (10 as the default value) frames. (2) there is another object overlapping with this object, and the IoU should be greater than Thr_{IoU} (0.2 as the default value). Secondly, we need to get the number of successfully attacked trajectories, for which the detected bounding box is no longer associated with the original tracklet after the attack. And the error state should last for more than dozens of frames (20 as the default value) or until the tracking of the attack object ends.

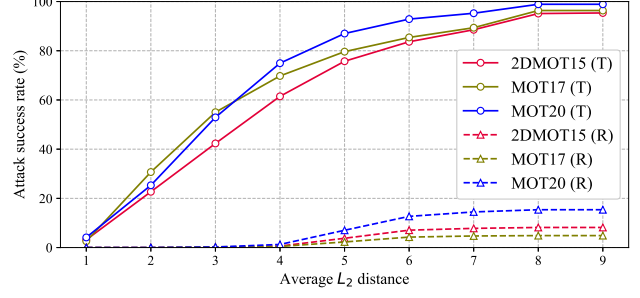
4.2. Adversarial Attack Results

We report the results of the single-target attack and multiple-target attack. The effectiveness and efficiency of our method are demonstrated through the attack success rate ($Succ.$ \uparrow), average attack frames ($\#Fm.$ \downarrow) and average L_2 distance (L_2 \downarrow) of the successful attacks.

Single-Target Attack. Single-target attack means that we only attack a specific trajectory. Tab. 1 shows the attack results on FairMOT and JDE using the three datasets. For a fair comparison, TraSw and RanAt have the same conditions of adding noises. To make the experiments more efficient, the addition of random noise in a tracklet is limited to 30 frames in FairMOT (50 in JDE). Figs. 4a and 4b show the variation of the attack success rate constrained by the attack frames or the perturbation of average L_2 distances. The attack performance of TraSw is significant, achieving much higher attack success rate ($Succ.$) by attacking less frames ($\#Fm.$) using smaller perturbations (L_2).



(a) Attack success rate at certain number of attacked frames



(b) Attack success rate at certain perturbation of L_2 distances

Figure 4. The evaluation results of trackers attacked by TraSw (T) or RanAt (R).

Table 1. Comparison on single-target attack.

Dataset	Tracker	Method	$Succ.$ \uparrow	$\#Fm.$ \downarrow	L_2 \downarrow
2DMOT15	FairMOT	RanAt	8.17%	9.97	5.07
		TraSw	95.37%	4.67	3.55
	JDE	RanAt	4.91%	9.11	4.99
		TraSw	89.34%	5.63	5.42
MOT17	FairMOT	RanAt	4.86%	9.34	5.01
		TraSw	96.35%	5.61	3.23
	JDE	RanAt	4.94%	12.08	5.20
		TraSw	90.49%	9.09	4.97
MOT20	FairMOT	RanAt	15.38%	7.71	5.18
		TraSw	98.89%	4.12	3.12
	JDE	RanAt	21.39%	14.49	5.14
		TraSw	95.19%	6.24	5.17

Table 2. Comparison on multiple target attack.

Dataset	Tracker	Method	$Succ.$ \uparrow	$Fm.$ \downarrow	L_2 \downarrow
2DMOT15	FairMOT	RanAt	27.32%	86.33%	5.03
		TraSw	81.95%	35.06%	2.79
	JDE	RanAt	28.72%	82.08%	5.02
		TraSw	95.96%	52.44%	3.98
MOT17	FairMOT	RanAt	25.00%	92.78%	5.03
		TraSw	82.01%	38.85%	2.71
	JDE	RanAt	44.20%	90.79%	5.03
		TraSw	97.54%	56.53%	3.99
MOT20	FairMOT	RanAt	62.37%	98.89%	5.03
		TraSw	82.02%	54.35%	3.28
	JDE	RanAt	82.10%	98.89%	5.03
		TraSw	99.68%	80.55%	5.45

Multiple-Target Attack. The experimental setting of multiple-target attack is the same as that of the single-target attack. Multiple-target attack means that all the trajectories satisfying the attack conditions will be attacked (Sec. 3.2). The performance of TraSw on each dataset is shown in Table 2. Unlike the single-target attack, here $Fm.$ represents the average ratio of attack frames in the video. It shows that we can make more than 80% tracklets fail to track with only about half of the video frames being attacked. The attack performance of TraSw is significant, achieving much higher attack success rate ($Succ.$) by attacking less ratio of attack frames ($Fm.$) using smaller perturbations (L_2).

4.3. Further Discussions

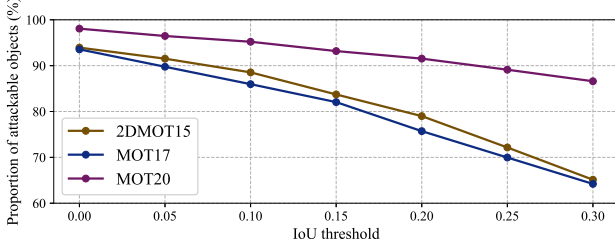
Ablation Study. We discuss the necessity of *PushPull* in Sec. 3.3, *CenterLeaping* in Sec. 3.4, and *adding failure noises* in Sec. 3.5. We conduct a series of comparison experiments on FairMOT to analyze and evaluate the contribution of each component in TraSw. The results are shown in Tab. 3. We can observe that each module has different degrees of importance on the two datasets. From the point of view of universality, it is beyond doubt that all the above

components are helpful.

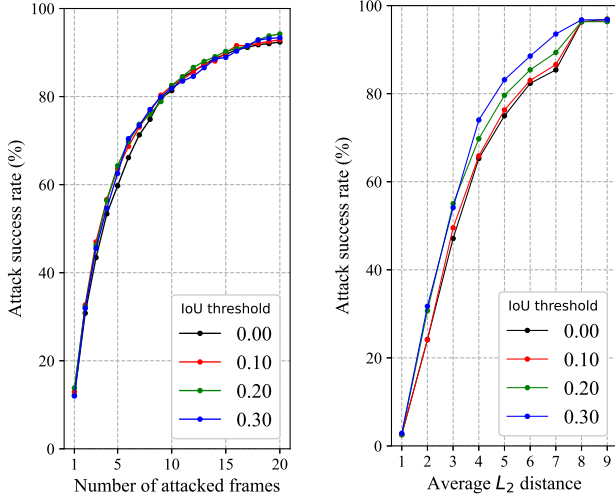
Table 3. Attack success rates at certain attack frames. P, C and F represent the *PullPush*, *CenterLeaping* and *Adding Failure Noise*, respectively. n_f presents n attacked frames.

Dataset	TraSw			Attack success rate (%)				
	P	C	F	1_f	5_f	10_f	15_f	20_f
2DMOT15	×	✓	✓	11.4	61.1	83.5	90.2	93.2
	✓	×	✓	11.2	67.1	87.6	91.6	94.5
	✓	✓	×	17.8	66.8	82.9	85.6	87.2
	✓	✓	✓	14.4	69.2	87.8	92.1	94.6
MOT17	×	✓	✓	9.7	51.1	75.0	85.9	90.0
	✓	×	✓	8.8	38.5	64.7	74.6	81.2
	✓	✓	×	15.5	62.3	79.3	85.9	89.1
	✓	✓	✓	13.8	64.3	82.5	90.3	94.2

Parameter Study on IoU Threshold. Our method attacks while finding two trajectories overlap with each other, and the IoU between them is greater than the threshold Thr_{IoU} . If Thr_{IoU} is set too high, we may not be able to find the attack targets in the video. If it is set too low, our method might not find the best opportunity to attack and need to attack more frames. Therefore, we analyze the impact of Thr_{IoU} , as shown in Fig. 5. The proportion of the



(a) Impact of Thr_{IoU}



(b) *Succ.* at certain attack frames

(c) *Succ.* at certain L_2 distances

Figure 5. Comparison on various threshold Thr_{IoU} . (a) shows the changes in the proportion of attackable objects. Representatively, the performance of TraSw on MOT17 test dataset under various Thr_{IoU} is shown in (b) and (c). We can observe that the performance of our method is affected by Thr_{IoU} . Considering the attack effectiveness and efficiency, we choose 0.2 as our Thr_{IoU} .

trajectories to be attacked decreases with the increasement of Thr_{IoU} .

Comparison with Object-Detection-Based Attack. Due to the detection branch in JDT based MOT trackers, object-detection-based attack method can also be used to fool the trackers. Hence, we choose a typical attack method against the object detection, which aims to make the attack object invisible to the object detection module. By comparison, we observe that our method is more effective than making the attack object invisible, as shown in Fig. 6.

Transferability to Detection-Based Tracker. As presented in Sec. 3, TraSw is designed for JDT-based MOT trackers. However, we find that it is also effective for TraSw to deceive tracklets in single-stage DBT-based MOT trackers while only *CenterLeaping* module can be used due to the only detection branch in DBT trackers. Specifically, we choose the SOTA DBT-based MOT tracker ByteTrack [32] as the target model. As same as attack on JDT-based MOT, there is no available attack method for the DBT-based MOT

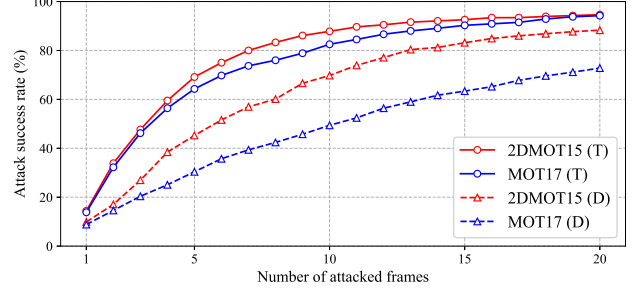


Figure 6. Evaluation results of FairMOT with TraSw (T) or object-detection-based attack method (D).

in the same scenario, we compare TraSw with the baseline of adding random noise. As shown in Tab. 4, we can see that the performance of TraSw in ByteTrack achieves an average success rate of over 91% with only a tiny increment on the L_2 distance.

Table 4. Attack on DBT (Single-Target).

Dataset	Tracker	Noise	<i>Succ.</i> \uparrow	$\#Fm.$ \downarrow	L_2 \downarrow
2DMOT15	ByteTrack	RanAt	5.90%	9.81	5.00
		TraSw	91.38%	4.45	6.48
MOT17	ByteTrack	RanAt	4.69%	8.55	5.19
		TraSw	92.91%	4.59	5.76

Noise Pattern. As shown in Fig. 7, obviously, the noise mainly focuses on the attack object and the screener object, leaving other regions almost not perturbed.

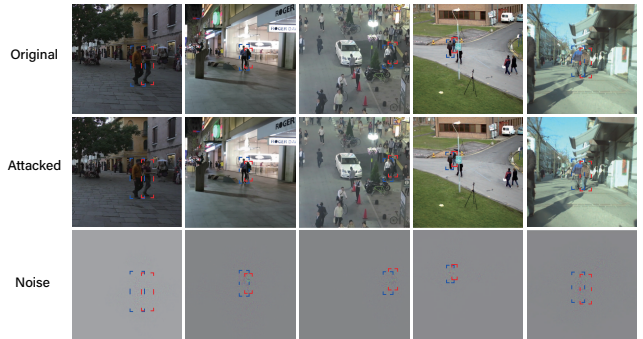


Figure 7. Five attack IDs from five different videos are randomly selected. The blue and red boxes represent the attack objects and the screener objects, respectively.

5. Conclusion

To our best knowledge, this is the first work to study the adversarial attack against JDT-based MOT trackers considering the complete tracking pipeline. We design an effective and efficient adversarial attack method that can deceive the

tracklets to fail to track using as few as one frame to attack the subsequent frames. The experimental results on standard benchmarks demonstrate that our method can fool the advanced trackers efficiently, and the failure in tracking also reveals the association algorithm’s weakness. We wish this work could inspire more works in designing robust MOT trackers and draw more attention to the adversarial attacks and defenses on MOT in the future.

References

- [1] Alex Bewley, Zongyuan Ge, Lionel Ott, Fabio Ramos, and Ben Upcroft. Simple online and realtime tracking. In *2016 IEEE International Conference on Image Processing (ICIP)*, pages 3464–3468, 2016. 1
- [2] Long Chen, Haizhou Ai, Zijie Zhuang, and Chong Shang. Real-time multiple people tracking with deeply learned candidate selection and person re-identification. In *2018 IEEE International Conference on Multimedia and Expo (ICME)*, pages 1–6, 2018. 1
- [3] Xuesong Chen, Xiyu Yan, Feng Zheng, Yong Jiang, Shu-Tao Xia, Yong Zhao, and Rongrong Ji. One-shot adversarial attacks on visual tracking with dual attention. In *Proceedings of the IEEE/CVF Conference on Computer Vision and Pattern Recognition (CVPR)*, pages 10176–10185, 2020. 3
- [4] Wongun Choi. Near-online multi-target tracking with aggregated local flow descriptor. In *Proceedings of the IEEE International Conference on Computer Vision (ICCV)*, pages 3029–3037, 2015. 1, 2
- [5] Francesco Croce and Matthias Hein. Reliable evaluation of adversarial robustness with an ensemble of diverse parameter-free attacks. In *Proceedings of the 37th International Conference on Machine Learning (ICML)*, pages 2206–2216, 2020. 3
- [6] Patrick Dendorfer, Hamid Rezaatoughi, Anton Milan, Javen Shi, Daniel Cremers, Ian Reid, Stefan Roth, Konrad Schindler, and Laura Leal-Taixé. MOT20: A benchmark for multi object tracking in crowded scenes. *arXiv preprint arXiv:2003.09003*, 2020. 6
- [7] Yinpeng Dong, Fangzhou Liao, Tianyu Pang, Hang Su, Jun Zhu, Xiaolin Hu, and Jianguo Li. Boosting adversarial attacks with momentum. In *Proceedings of the IEEE Conference on Computer Vision and Pattern Recognition (CVPR)*, pages 9185–9193, 2018. 3
- [8] Yinpeng Dong, Hang Su, Baoyuan Wu, Zhifeng Li, Wei Liu, Tong Zhang, and Jun Zhu. Efficient decision-based black-box adversarial attacks on face recognition. In *Proceedings of the IEEE/CVF Conference on Computer Vision and Pattern Recognition (CVPR)*, pages 7714–7722, 2019. 1
- [9] Kaiwen Duan, Song Bai, Lingxi Xie, Honggang Qi, Qingming Huang, and Qi Tian. Centernet: Keypoint triplets for object detection. In *Proceedings of the IEEE/CVF International Conference on Computer Vision (ICCV)*, pages 6569–6578, 2019. 3
- [10] Ian J Goodfellow, Jonathon Shlens, and Christian Szegedy. Explaining and harnessing adversarial examples. *arXiv preprint arXiv:1412.6572*, 2014. 3
- [11] Jan Hendrik Metzen, Mummadi Chaithanya Kumar, Thomas Brox, and Volker Fischer. Universal adversarial perturbations against semantic image segmentation. In *Proceedings of the IEEE international conference on computer vision*, pages 2755–2764, 2017. 1
- [12] Shuai Jia, Yibing Song, Chao Ma, and Xiaokang Yang. IoU attack: Towards temporally coherent black-box adversarial attack for visual object tracking. In *Proceedings of the IEEE/CVF Conference on Computer Vision and Pattern Recognition (CVPR)*, pages 6709–6718, 2021. 3
- [13] Yunhan Jia, Yantao Lu, Junjie Shen, Qi A Chen, Zhenyu Zhong, and Tao Wei. Fooling detection alone is not enough: First adversarial attack against multiple object tracking. In *International Conference on Learning Representations (ICLR)*, 2020. 2, 3
- [14] Laura Leal-Taixé, Anton Milan, Ian Reid, Stefan Roth, and Konrad Schindler. MOTChallenge 2015: Towards a benchmark for multi-target tracking. *arXiv preprint arXiv:1504.01942*, 2015. 6
- [15] Bo Li, Wei Wu, Qiang Wang, Fangyi Zhang, Junliang Xing, and Junjie Yan. Siamrpn++: Evolution of siamese visual tracking with very deep networks. In *Proceedings of the IEEE/CVF Conference on Computer Vision and Pattern Recognition (CVPR)*, pages 4282–4291, 2019. 3
- [16] Bo Li, Junjie Yan, Wei Wu, Zheng Zhu, and Xiaolin Hu. High performance visual tracking with siamese region proposal network. In *Proceedings of the IEEE Conference on Computer Vision and Pattern Recognition (CVPR)*, pages 8971–8980, 2018. 3
- [17] Siyuan Liang, Baoyuan Wu, Yanbo Fan, Xingxing Wei, and Xiaochun Cao. Parallel rectangle flip attack: A query-based black-box attack against object detection. In *Proceedings of the IEEE/CVF International Conference on Computer Vision (ICCV)*, pages 7697–7707, 2021. 1, 2
- [18] Jiadong Lin, Chuanbiao Song, Kun He, Liwei Wang, and John E Hopcroft. Nesterov accelerated gradient and scale invariance for adversarial attacks. In *International Conference on Learning Representations (ICLR)*, 2020. 3
- [19] Wenhan Luo, Junliang Xing, Anton Milan, Xiaoqin Zhang, Wei Liu, and Tae-Kyun Kim. Multiple object tracking: A literature review. *Artificial Intelligence*, page 103448, 2020. 1, 2
- [20] Aleksander Madry, Aleksandar Makelov, Ludwig Schmidt, Dimitris Tsipras, and Adrian Vladu. Towards deep learning models resistant to adversarial attacks. In *International Conference on Learning Representations (ICLR)*, 2018. 3
- [21] Anton Milan, Laura Leal-Taixé, Ian Reid, Stefan Roth, and Konrad Schindler. MOT16: A benchmark for multi-object tracking. *arXiv preprint arXiv:1603.00831*, 2016. 1, 2, 6
- [22] Anh Nguyen, Jason Yosinski, and Jeff Clune. Deep neural networks are easily fooled: High confidence predictions for unrecognizable images. In *Proceedings of the IEEE Conference on Computer Vision and Pattern Recognition (CVPR)*, pages 427–436, 2015. 1
- [23] Florian Schroff, Dmitry Kalenichenko, and James Philbin. FaceNet: A unified embedding for face recognition and clustering. In *Proceedings of the IEEE Conference on Com-*

- puter Vision and Pattern Recognition (CVPR), pages 815–823, 2015. 4
- [24] Christian Szegedy, Wojciech Zaremba, Ilya Sutskever, Joan Bruna, Dumitru Erhan, Ian J. Goodfellow, and Rob Fergus. Intriguing properties of neural networks. In *International Conference on Learning Representations (ICLR)*, 2014. 1, 3
 - [25] Zhongdao Wang, Liang Zheng, Yixuan Liu, Yali Li, and Shengjin Wang. Towards real-time multi-object tracking. In *European Conference on Computer Vision (ECCV)*, pages 107–122, 2020. 1, 2, 3, 6
 - [26] Xingxing Wei, Siyuan Liang, Ning Chen, and Xiaochun Cao. Transferable adversarial attacks for image and video object detection. *arXiv preprint arXiv:1811.12641*, 2018. 1, 2
 - [27] Nicolai Wojke, Alex Bewley, and Dietrich Paulus. Simple online and realtime tracking with a deep association metric. In *2017 IEEE International Conference on Image Processing (ICIP)*, pages 3645–3649, 2017. 1
 - [28] Cihang Xie, Jianyu Wang, Zhishuai Zhang, Yuyin Zhou, Lingxi Xie, and Alan Yuille. Adversarial examples for semantic segmentation and object detection. In *Proceedings of the IEEE International Conference on Computer Vision (ICCV)*, pages 1369–1378, 2017. 1, 2
 - [29] Bin Yan, Dong Wang, Huchuan Lu, and Xiaoyun Yang. Cooling-shrinking attack: Blinding the tracker with imperceptible noises. In *Proceedings of the IEEE/CVF Conference on Computer Vision and Pattern Recognition (CVPR)*, pages 990–999, 2020. 3
 - [30] Bangjie Yin, Wenxuan Wang, Taiping Yao, Junfeng Guo, Zelun Kong, Shouhong Ding, Jilin Li, and Cong Liu. Adv-Makeup: A new imperceptible and transferable attack on face recognition. In *Proceedings of the Thirtieth International Joint Conference on Artificial Intelligence, (IJCAI)*, pages 1252–1258, 2021. 1
 - [31] Fengwei Yu, Wenbo Li, Quanquan Li, Yu Liu, Xiaohua Shi, and Junjie Yan. Poi: Multiple object tracking with high performance detection and appearance feature. In *European Conference on Computer Vision (ECCV)*, pages 36–42, 2016. 1, 2
 - [32] Yifu Zhang, Peize Sun, Yi Jiang, Dongdong Yu, Zehuan Yuan, Ping Luo, Wenyu Liu, and Xinggang Wang. ByteTrack: Multi-object tracking by associating every detection box. *arXiv preprint arXiv:2110.06864*, 2021. 2, 8
 - [33] Yifu Zhang, Chunyu Wang, Xinggang Wang, Wenjun Zeng, and Wenyu Liu. Fairmot: On the fairness of detection and re-identification in multiple object tracking. *International Journal of Computer Vision (IJCV)*, pages 1–19, 2021. 1, 2, 3, 6
 - [34] Xingyi Zhou, Vladlen Koltun, and Philipp Krähenbühl. Tracking objects as points. In *European Conference on Computer Vision (ECCV)*, pages 474–490, 2020. 1, 2